

Origin of recoil hysteresis loops in Sm–Co/Fe exchange-spring magnets

Y. Choi,^{a)} J. S. Jiang, J. E. Pearson, and S. D. Bader
Materials Science Division, Argonne National Laboratory, Argonne, Illinois 60439

J. P. Liu
Department of Physics, University of Texas at Arlington, Arlington, Texas 76019

(Received 30 April 2007; accepted 5 June 2007; published online 10 July 2007)

Open recoil loops are often interpreted as a consequence of a breakdown in exchange coupling and attributed to the decoupled soft phase in exchange-coupled permanent magnets. However, in element-specific recoil loop measurements on Sm–Co/Fe exchange spring magnets, the authors found that the open recoil loops were present not only in the soft (Fe) layer but also in the hard (Sm–Co) layer, and were not a consequence of exchange coupling breakdown between the soft and hard layers. Comparison between the experimental results and micromagnetic calculations reveals that the observed open recoil loops originate from the anisotropy variations in the Sm–Co layer.

© 2007 American Institute of Physics. [DOI: 10.1063/1.2752534]

By combining the high magnetic anisotropy of a magnetically hard phase and the high saturation moment of a magnetically soft phase, exchange-coupled nanocomposite permanent magnets can have magnetic properties that are superior to those of single-phase magnets.^{1,2} In nanocomposite magnets, the exchange coupling between the two phases is the principal mechanism of their enhanced maximum energy product values.¹ Therefore, understanding the nature of magnetic interactions at the interface is important for designing nanocomposite magnets with optimal hard magnetic properties.

Recoil measurements have been often used to characterize exchange-coupled nanocomposite permanent magnets because the recoil characteristics are sensitive to interphase conditions, as demonstrated by previous studies.^{3–10} Recoil loops are measured by removing and reapplying a demagnetizing field to a magnetic material, as the demagnetizing field is increased successively. Open recoil loops refer to the situation where the magnetizing and demagnetizing branches do not overlap, thereby enclosing an area. Time-independent open recoil loops are usually interpreted as a sign of incomplete exchange coupling. Since open recoil loops are typically absent in single-phase magnets, the presence of open recoil loops is seen as a manifestation of breakdown in the exchange coupling and the enclosed area is attributed to the decoupled volume in the soft phase.^{5–10} In addition, other factors, such as coercivity distribution and the volume fraction of the constituent phases, are also found to be important in understanding the origin of open recoil loops.¹¹

In the present work, we report element-resolved recoil hysteresis loops from Sm–Co/Fe exchange-spring magnet films^{1,2} in addition to bulk magnetometry measurements and micromagnetic simulations. The exchange-spring bilayer structure^{12,13} provides a convenient system to study fundamental properties since individual layer thickness can be controlled. Using x-ray resonant magnetic scattering (XRMS) magnetometry,¹⁴ we extracted recoil loops from the Fe and Sm–Co layers separately. The measurements show that open recoil loops are present not only in the soft phase layer but also in the hard phase layer. Our experimental and

simulation results reveal that the onset of the open recoil loops is not necessarily a direct consequence of exchange coupling breakdown between the two phases but rather originates from variations in the Sm–Co layer anisotropy.

Two epitaxial Sm–Co/Fe exchange-spring bilayer samples with in-plane uniaxial anisotropy were fabricated using magnetron sputtering, as described in Refs. 13 and 15. Sm–Co layers with a nominal Sm₂Co₇ composition were grown on MgO(110) substrates with an epitaxial Cr(211) buffer layer. For one sample (labeled T100), the Fe layer was deposited at 100 °C. For the other sample (labeled T400), the Fe layer was deposited at 400 °C to increase the interdiffusion at the Sm–Co/Fe interface. Thus, any differences in the magnetic behaviors between the two are expected to be caused by the modifications near the Sm–Co/Fe interfacial region.

Recoil loops were measured on the samples with vibrating sample magnetometry (VSM), as shown in Fig. 1. The recoil measurements show open areas enclosed by the demagnetizing and recoil curves, indicating the presence of irreversible processes during the recoil measurements. The major demagnetizing curves show that the nucleation field is increased and the irreversible switching field is decreased for the T400 sample, in comparison with the T100 sample. These characteristic changes are attributed to an enhanced exchange coupling effectiveness due to interdiffusion.¹⁶ Changes in the recoil loop areas coincide with the enhanced effective exchange coupling between the two layers. This correlation between the open area and the effectiveness in

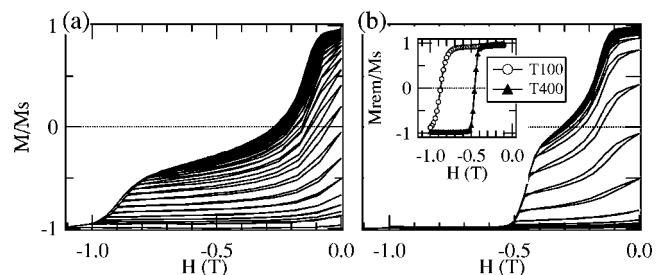


FIG. 1. Easy axis demagnetizing curve and recoil loops measured at 300 K for the (a) T100 and (b) T400 samples. The inset shows normalized remanence curves.

^{a)}Electronic mail: yschoi@anl.gov

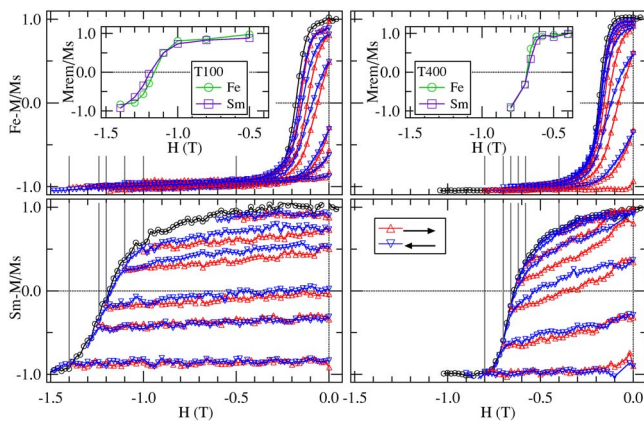


FIG. 2. (Color online) Element-specific recoil loops from the T100 and T400 samples at 200 K. The dotted vertical lines indicate the initial field for each recoil curve. The major demagnetization curves (with circle symbol) are shown as a reference. Normalized remanence curves from the Fe and Sm recoil curves are shown as insets.

exchange coupling led to the use of the area of the recoil loop as a measure of the strength of the exchange coupling.^{5–10}

While the VSM results provide the aggregate magnetic response from the samples, the XRMS magnetometry provides the magnetization behavior of each layer separately. The XRMS measurements were performed at beamline 4ID-C of the Advanced Photon Source at Argonne National Laboratory.¹⁷ The XRMS measurements were made at the Fe L_3 and Sm M_4 absorption edges to probe the Fe and Sm–Co layers, respectively. Element-specific recoil magnetization hysteresis loops were obtained by collecting the asymmetry ratio¹⁸ at 200 K as a function of external magnetic field H at a fixed x-ray energy and specular angle ($\sim 10^\circ$). At low angles, the XRMS signal is sensitive to the response only from the top portion of the Fe or Sm–Co layers due to x-ray absorption effect. To estimate the probing depth in our XRMS measurements, we calculated an electric field intensity profile inside the film layers for each measurement.^{15,19} Based on the calculations, 80% of the measured XRMS signals are from the top 5 nm of the 20 nm thick Fe layer (near the Fe/cap interface) and the top 10 nm of the 20 nm thick Sm–Co layer (near the Sm–Co/Fe interface).

The element-specific recoil loops from the two samples are shown in Fig. 2. When the magnitude of the applied demagnetizing field is small, both Fe and Sm recoil curves are completely reversible. As the demagnetizing field increases in magnitude, enclosed areas appear in both Fe and Sm recoil loops. Moreover, the areas appear and disappear concurrently in the two layers. The area enclosed by a recoil loop persists until the demagnetizing field is much greater than the coercive field of the Sm major loop. Open recoil loops, measured by bulk magnetometry, as in Fig. 1, are often attributed to the decoupled soft phase.^{5–8} In contrast, our element-specific measurements show that the open recoil loops are present not only in the soft (Fe) layer but also in the hard (Sm–Co) layer in our two samples that have different interface morphologies and exchange coupling effectiveness.

In Fig. 2, the major Sm-demagnetization curve from the T400 sample shows more abrupt changes, indicating that the switching field distribution of the Sm–Co layer is narrower than that of the T100 sample. The different distributions contribute to the observed difference between the recoil

loops from the two samples. Overall, the open recoil loops from the T400 sample are thicker (larger ΔM) since a higher fraction of the Sm–Co volume is perturbed by a given demagnetizing field, in comparison with the T100 sample. Otherwise, the open recoil loops from the two samples are similar in terms of their overall behavior. The exchange coupling effectiveness between the Fe and Sm–Co does influence the open recoil loops since it affects the switching field distribution. However, the exchange coupling does not appear to have a simple correlation with the open recoil loops.

In Fig. 2, normalized remanence curves from the element-specific recoil loops are shown as insets. For each sample, the Fe remanence curve mimics its Sm counterpart. This behavior is striking, considering the Fe volume responsible for the measured Fe XRMS recoil loops is spatially separated from the Sm–Co volume responsible for the Sm XRMS recoil loops. This result indicates that the presence of the open recoil loops may not be a consequence of a breakdown in interphase exchange coupling. If the breakdown were associated with open recoil loops, the top region of the Fe layer, which contributes most to the XRMS curves while being the farthest from the Sm–Co/Fe interface, would be the first region to become decoupled and reversible again.

As shown in Fig. 2, the Fe layer becomes irreversible and open recoil loops appear in both layers only after the demagnetizing field is sufficiently high to initiate magnetization reversal in the Sm–Co layer. This suggests that the open recoil loops are related to domain formation in the Sm–Co layer. Moreover, the similarity between the Fe and Sm remanence curves suggests that, at $H=0$, the Fe layer mirrors the domain configuration in the Sm–Co layer below with the same area fraction of the reversed domains. One of the possible origins of this partial reversal is anisotropy variations in the hard layer. A previous study using high-resolution electron microscopy had shown that similarly grown nominally Sm_2Co_7 films contained a mixture of SmCo_3 and SmCo_5 phases due to stacking disorder along the c axis.²⁰ There may be some weak Sm–Co grains with different anisotropy values in our films as well.

To illustrate that a distribution in hard phase anisotropy would give rise to the kind of hysteretic recoil behavior observed in our XRMS measurements, we simulated recoil measurements on the same Sm–Co/Fe bilayer structure using micromagnetic calculations.²¹ Figure 3(a) shows the model Sm–Co/Fe structure for our simulations. The model includes three weak Sm–Co grains with reduced magnitudes of Sm–Co anisotropy. The simulated volume is $L_x \times L_y \times L_z = 300 \times 300 \times 40 \text{ nm}^3$ with periodic conditions in the x and y directions. The simulation cell size was $1 \times 300 \times 1 \text{ nm}^3$ so that the anisotropy value was varied in the x and z directions only. The anisotropy values of the three weak Sm–Co grains are 22%, 21%, and 20% of the nominal value $K_0 = 5 \times 10^7 \text{ erg/cm}^3$. Meanwhile other parameters are fixed using the parameters from Ref. 13, i.e., there is no weakening of the exchange coupling between the Fe and Sm–Co layers, or between the normal and weak Sm–Co grains.²²

In Fig. 3(g), the total and the individual Fe and Sm–Co layer contributions are plotted separately. Consistent with our XRMS experimental results, the open recoil loops are present in both layers with the same remanence values for both layers. As the demagnetizing field H increases, the Fe layer reverses its magnetization first [Fig. 3(b)]. Magnetization reversal initiates in the Sm–Co grain with the smallest

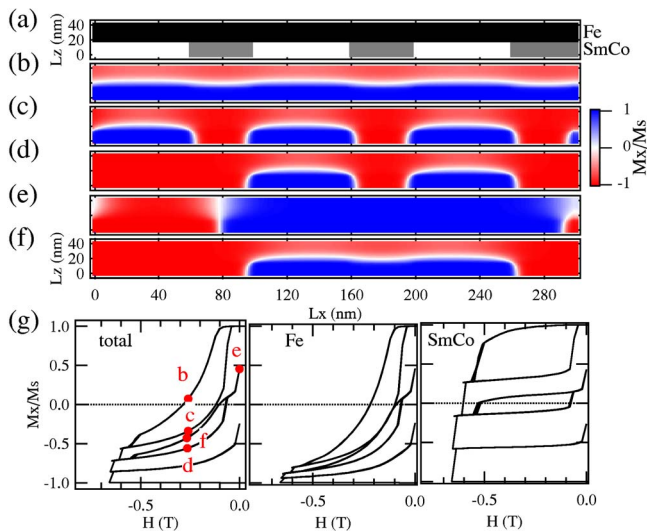


FIG. 3. (Color online) (a) Model Sm–Co/Fe structure containing three weak Sm–Co grains marked in gray. [(b)–(f)] Simulated magnetic configurations at different fields as indicated in (g). (g) Simulated recoil loops for the total, Fe and Sm–Co layers.

anisotropy value. Eventually the rest of weak Sm–Co grains reverse, and as H is reduced back to zero, portions of the Fe layer and the weak Sm–Co grains reverse back to the original direction [Fig. 3(c)]. As a result of the different demagnetizing and recoil paths, the recoil loop becomes open for the Fe and Sm–Co layers. However, this type of recoil loops does not lead to reduced remanence values. In Figs. 3(d)–3(f), the Fe and Sm–Co remanence values reduce as observed experimentally. This irreversible change occurs as the lateral domain walls collapse together along with the Fe region above, as shown in Fig. 3(e). In real samples with a much larger number of grains and with anisotropy distributions, this type of domain wall collapsing would occur continuously during a recoil measurement, contributing to multiple open recoil loops as seen in Figs. 1 and 2.

The domain nucleation in the hard layer can be considered as a consequence of the coupling breakdown between Sm–Co grains. However, this *breakdown* is inherently different from an interphase coupling breakdown. Thus, it is important to recognize that routine open recoil loop measurements on nanocomposite magnets do not provide straightforward information about the extent of interphase exchange couplings, as evidenced by the comparison between our two samples.

Using an element-sensitive magnetic characterization technique, we have measured recoil loops on exchange-coupled nanocomposite magnets. Our element-resolved re-

coil loop measurements provide clues about the origin of open recoil loops that are typically measured with conventional magnetometry. The experimental and micromagnetic simulation results indicate that the open recoil loops are linked to variations in the hard layer anisotropy rather than to a breakdown in interphase exchange coupling.

This work was supported by ONR/MURI under Grant No. N00014-05-1-0497 and by U.S. Department of Energy, Office of Science, under Contract No. DE-AC02-06CH11357.

- ¹E. F. Kneller and R. Hawig, IEEE Trans. Magn. **27**, 3588 (1991).
- ²R. Skomski and J. M. D. Coey, Phys. Rev. B **48**, 15812 (1993).
- ³M. Emura, D. R. Cornejo, and F. P. Missell, J. Appl. Phys. **87**, 1387 (2000).
- ⁴E. H. Feuttrill, P. G. McCormick, and R. Street, J. Phys. D **29**, 2320 (1996).
- ⁵D. Goll, M. Seeger, and H. Kronmüller, J. Magn. Magn. Mater. **185**, 49 (1998).
- ⁶D. C. Crew, J. Kim, L. H. Lewis, and K. Barmak, J. Magn. Magn. Mater. **233**, 257 (2001).
- ⁷C. L. Harland, L. H. Lewis, Z. Chen, and B.-M. Ma, J. Magn. Magn. Mater. **271**, 53 (2004).
- ⁸K. Kang, L. H. Lewis, J. S. Jiang, and S. D. Bader, J. Appl. Phys. **98**, 113906 (2005).
- ⁹A. Bollero, O. Gutfleisch, K.-H. Müller, L. Schultz, and G. Drazic, J. Appl. Phys. **91**, 8159 (2002).
- ¹⁰J. Zhang, Y. K. Takahashi, R. Gopalan, and K. Hono, Appl. Phys. Lett. **86**, 122509 (2005).
- ¹¹R. William McCallum, J. Magn. Magn. Mater. **299**, 472 (2006).
- ¹²K. Mibu, T. Nagahama, T. Shinjo, and T. Ono, Phys. Rev. B **58**, 6442 (1998).
- ¹³E. E. Fullerton, J. S. Jiang, and S. D. Bader, J. Magn. Magn. Mater. **200**, 392 (1999).
- ¹⁴J. W. Freeland, K. Bussmann, P. Lubitz, Y. U. Idzerda, and C.-C. Kao, Appl. Phys. Lett. **73**, 2206 (1998).
- ¹⁵Y. Choi, J. S. Jiang, Y. Ding, R. A. Rosenberg, J. E. Pearson, S. D. Bader, A. Zambano, M. Murakami, I. Takeuchi, Z. L. Wang, and J. P. Liu, Phys. Rev. B **75**, 104432 (2007).
- ¹⁶J. S. Jiang, J. E. Pearson, Z. Y. Liu, B. Kabius, S. Trasobares, D. J. Miller, S. D. Bader, D. R. Lee, D. Haskel, G. Srajer, and J. P. Liu, Appl. Phys. Lett. **85**, 5293 (2004).
- ¹⁷J. W. Freeland, J. C. Lang, G. Srajer, R. Winarski, D. Shu, and D. M. Mills, Rev. Sci. Instrum. **73**, 1408 (2001).
- ¹⁸The asymmetry ratio is defined as $(I^+ - I^-)/(I^+ + I^-)$, where I^{\pm} are the scattered intensities measured for the two opposite circular polarizations of the incoming x rays. The field was applied along the easy axis in the film plane at a fixed field sweep rate.
- ¹⁹L. G. Parratt, Phys. Rev. **95**, 359 (1954).
- ²⁰M. Benaissa, K. M. Krishnan, E. E. Fullerton, and J. S. Jiang, IEEE Trans. Magn. **34**, 1204 (1998).
- ²¹The LLG micromagnetics simulator (<http://llgmicro.home.mindspring.com>).
- ²²Variations in these exchange coupling constants did not reproduce open recoil loops.